DTIC FILE COPY

PHOTOGRAPH THIS SHEET

AD-A220 066

DTIC ACCESSION NUMBER

LEVEL

INVENTORY

1

HDL-TR-2165

DOCUMENT IDENTIFICATION

Aug 1989

DISTRIBUTION STATEMENT A
Approved for public release;
Distribution Unlimited

DISTRIBUTION STATEMENT

ACCESSION FOR

NTIS GRA&I X
DTIC TRAC ☐
UNANNOUNCED ☐
JUSTIFICATION

BY

DISTRIBUTION/

AVAILABILITY CODES

| DISTRIBUTION | AVAILABILITY AND/OR SPECIAL | |
|---|---|---|
| A-1 | | |

DISTRIBUTION STAMP

DTIC ELECTE APR 04 1990 S E D

DATE ACCESSIONED

DATE RETURNED

90 04 04 001

DATE RECEIVED IN DTIC

REGISTERED OR CERTIFIED NUMBER

PHOTOGRAPH THIS SHEET AND RETURN TO DTIC-FDAC

DTIC FORM APR 87 70A

DOCUMENT PROCESSING SHEET

PREVIOUS EDITIONS MAY BE USED UNTIL STOCK IS EXHAUSTED

① TCE

HDL-TR-2165



# Spectral Properties of a 1.3-μm InGaAsP Diode Laser Under Direct Modulation

– (U)

by Fred Semendy and
Emanuel Kaizen

④ 1/87 - 2/88 ; 8/89



U.S. Army Laboratory Command
③ Harry Diamond Laboratories
Adelphi, MD 20783-1197
(HDL)



This report covers TI number(s) None
Technical Information

# REPORT DOCUMENTATION PAGE

Form Approved OMB No. 0704-0188

| | |
|---|---|
| 1a. REPORT SECURITY CLASSIFICATION<br>Unclassified | 1b. RESTRICTIVE MARKINGS |
| 2a. SECURITY CLASSIFICATION AUTHORITY | 3. DISTRIBUTION/AVAILABILITY OF REPORT<br>Approved for public release; distribution unlimited. |
| 2b. DECLASSIFICATION/DOWNGRADING SCHEDULE | |
| 4. PERFORMING ORGANIZATION REPORT NUMBER(S)<br>HDL-TR-2165 | 5. MONITORING ORGANIZATION REPORT NUMBER(S) |
| 6a. NAME OF PERFORMING ORGANIZATION<br>Harry Diamond Laboratories<br>6b. OFFICE SYMBOL (if applicable)<br>SLCHD-ST-OP | 7a. NAME OF MONITORING ORGANIZATION |
| 6c. ADDRESS (City, State, and ZIP Code)<br>2800 Powder Mill Road<br>Adelphi, MD 20783-1197 | 7b. ADDRESS (City, State, and ZIP Code) |
| 8a. NAME OF FUNDING/SPONSORING ORGANIZATION<br>U.S. Army Laboratory Command<br>7b. OFFICE SYMBOL (if applicable)<br>AMSLC | 9. PROCUREMENT INSTRUMENT IDENTIFICATION NUMBER |
| 8c. ADDRESS (City, State, and ZIP Code)<br>2800 Powder Mill Road<br>Adelphi, MD 20783-1145 | 10. SOURCE OF FUNDING NUMBERS<br>PROGRAM ELEMENT NO.: P611102.H4400<br>PROJECT NO.: AH44<br>TASK NO.:<br>WORK UNIT ACCESSION NO.: |

11. TITLE (Include Security Classification)
Spectral Properties of a 1.3-μm InGaAsP Diode Laser Under Direct Modulation

12. PERSONAL AUTHOR(S)
Fred Semendy and Emanuel Katzen

| 13a. TYPE OF REPORT | 13b. TIME COVERED | 14. DATE OF REPORT (Year, Month, Day) | 15. PAGE COUNT |
|---|---|---|---|
| Final | FROM 9/87 TO 2/88 | August 1989 | 18 |

16. SUPPLEMENTARY NOTATION
AMS code: 611102.H440011, HDL project: AE1951

| 17. COSATI CODES | | | 18. SUBJECT TERMS (Continue on reverse if necessary and identify by block number) |
|---|---|---|---|
| FIELD | GROUP | SUB-GROUP | High frequency, direct current modulation, high-speed diode lasers, InGaAsP, fast detectors, nonlinear gain effects, modulation index, FM properties |

19. ABSTRACT (Continue on reverse if necessary and identify by block number)

Direct modulation of a buried heterostructure (BH) InGaAsP laser diode was performed up to 18 GHz, and FM properties were observed. The number of lasing modes increased with increasing modulation depth. For a given rf power, the FM index went from 0.7 to 0 as the modulation frequency was increased. These measurements indicate that the nonlinear gain effects mainly influence the modulation characteristics of this laser, and wider bandwidths and modulation indexes can be achieved in this type of multimode device.

| | |
|---|---|
| 20. DISTRIBUTION/AVAILABILITY OF ABSTRACT<br>☐ UNCLASSIFIED/UNLIMITED ☒ SAME AS RPT. ☐ DTIC USERS | 21. ABSTRACT SECURITY CLASSIFICATION<br>Unclassified |
| 22a. NAME OF RESPONSIBLE INDIVIDUAL<br>John M. Pelligrino | 22b. TELEPHONE (Include Area Code)<br>(202) 394-2520<br>22c. OFFICE SYMBOL<br>SLCHD-ST-OP |

## Contents

Page



## Figures

# 1. Introduction

The high-frequency modulation of diode lasers has been a subject of active research for signal transmission in digital and analog fiberoptic communications, fiberoptic links, delay lines, and phased array beam steering. Recently high-frequency intensity modulation of InGaAsP has achieved bandwidths of 23 GHz [1-2]. The widespread use of semiconductor lasers for microwave fiberoptic links has stimulated interest in the investigation of spectral characteristics of these devices under high-frequency modulation.

Spectrum broadening with increased lasing modes and definite enhancement under high-speed modulation conditions were first pointed out for GaAs lasers [3]. This broadening can drastically reduce the transmission bandwidths of optical communication systems because of material dispersion in the fiber. It has been observed that the wavelength of a single longitudinal mode shifts and broadens with changes in modulation current for the same frequency of modulation [4-5]. This behavior is referred to as dynamic wavelength or frequency shift and is a major obstacle preventing the realization of an ultra-high-quality communication system [6]. The dynamic line broadening with current modulation is due to the variations in carrier density, resulting in refractive index changes which cause oscillation frequency shifts [7]. The dynamic line broadening from frequency chirping is intrinsic to any laser diode, and it may be possible to use controlled chirping to achieve pulse compression and dispersionless transmission in optical fibers to overcome this problem.

This report gives an account of spectral modulation characteristics of a GTE 1.3-μm InGaAsP vapor-phase-regrown buried-heterostructure (VPR-BH) laser under modulation in the 2- to 18-GHz range. The modulation depth and signal outputs were monitored with fast photodiodes and a fast oscilloscope.

# 2. Experimental Setup

Figure 1 shows the setup used to study the spectral modulation characteristics. The setup consists of the following: GTE InGaAsP laser diode, current supply, temperature controller, bias tee, rf power supply, tuner, beam splitters (BS), Spex 1701 grating spectrometer, Burleigh RC-60 scanning Fabry-Perot (FP) interferometer, ultra-high-speed InGaAs/InP photodetector (PD) made by GTE, digital voltmeter, amplifier, other types of PIN diodes, X-Y plotter, oscilloscope, and spectrum analyzer. The laser generally gives a multimode spectrum for a given current above the threshold and therefore it is important to use a grating spectrometer to select a single laser mode with high resolution. The FP interferometer measures fine frequency shifts and displays the details of the optical spectra with a free spectral range of 15 GHz. The sweep mode of the FP has the advantage of showing the dynamic spectral changes on the oscilloscope. One of the beams split by the second beamsplitter is made to fall on the extremely fast photodetector and the detected frequency is measured with the spectrum analyzer. The other beam is detected by a PIN detector and the output is plotted.

**Figure 1. Experimental setup.**

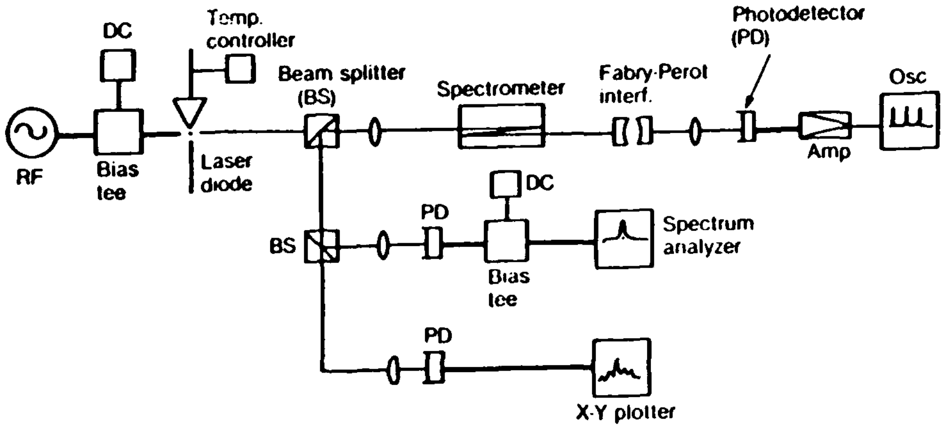


# 3. Theory

Rate equations are used to describe the carrier and photon density of semiconductor lasers. The generalized multimode rate equations which can be applied to a single mode case [8-9] are given by

$$\frac{dN}{dt} = \frac{I}{eV} - R(N) - v_g \tau \sum_i g_i S_i \tag{1}$$

and

$$\frac{dS_i}{dt} = v_g\left(\tau_{gi} - \alpha_T\right) S_i \ , \tag{2}$$

where $N$ is the carrier density, $I$ is the injection current, $e$ is the electron charge, $V$ is the active layer volume, $R(N)$ is the total recombination rate, $v_g$ is the photon group velocity, t is the confinement factor, $S_i$ is the photon density in the longitudinal mode $i$, $g_i$ is the net gain of mode $i$, and $a_T$ is the optical loss. Spontaneous emission has negligible contribution into the lasing mode and is therefore omitted for analysis above the lasing threshold. The net gain, $g_i$, which is the sum of a linear term, $G(N)$, including the parabolicity factor, $\Delta G$, and a generalized nonlinear term, $\Sigma \varepsilon_{ij} S_j$, with parameter $\varepsilon_{ij}$ is given by

$$g_i = G(N) - \Delta G_i^2 - \sum_j \varepsilon_{ij} S_j \ . \tag{3}$$

From frequency modulation index measurements it can be directly verified that the gain saturation term $\Sigma \varepsilon_{ij} S_j$ is present and makes the dominant contribution to the intensity modulation factor.

The total photon density modulation response $(\Delta S)^2$ with a frequency $\omega$ is given by

$$(\Delta S)^2 = \left(\frac{1}{eV} \frac{\delta I}{v_g \alpha_T}\right)^2 \left[\frac{\omega_0^4}{(\omega_s^2 - \omega^2)^2 + \gamma^2 \omega^2}\right] , \tag{4}$$

where the resonant frequency, $\omega_0$, is described by

$$\omega_0^2 = v_g^2 \tau \alpha_T \frac{dG}{dN} S \ , \tag{5}$$

where dG/dN is the differential gain and $S = \Sigma_i S_i$. The damping factor, $\gamma$, is given by

$$\gamma = \frac{1}{\tau_c} + \frac{\omega_0^2}{v_g \alpha_T} + \gamma_n \tag{6}$$

and

$$\gamma_n = v_g + \sum_i \sum_j \varepsilon_{ij} \theta_i \theta_j S \ , \tag{7}$$

where $\tau_c = [1/(\partial R/\partial N)]$ is the differential carrier lifetime at the lasing threshold, $\theta_i = S_i/S$ is the normalized photon density in mode $i$, and $S$ is the total photon density.

The resonance frequency and damping factor play an important role in determining the dynamic response of the diode lasers. However, it is widely known that the dynamic response of InGaAsP diode lasers cannot be predicted [10-12] by use of the laser rate equation with only the linear gain term. The relaxation oscillation damping due to the linear term alone is much weaker. Therefore, to account for the strong damping, other nonlinear effects must be taken into consideration.

Assuming that the device is under sinusoidal small signal modulation, $\Delta S = (\Delta S)_0 e^{i\omega t}$ at a total bias photon density $S$. Performing small signal analysis on equations (1) and (2) with the assumption that $d\Delta G/dN$ is negligible, we get the following:

$$\delta N = \left( vg\tau \frac{dG}{dN} \right)^{-1} (i\omega + \gamma_n) \frac{\Delta S}{S} \ , \tag{8}$$

where $\delta N$ is described by the total photon density modulation. Here the gain change $dG/dN$ is numerically larger than the wavelength dependent gain change from the longitudinal modes.

The incremental optical frequency change $\Delta\gamma$ is related to the carrier density change [13] by

$$\frac{\Delta v}{v} = \frac{\tau}{n_g} \frac{dn'}{dN} \delta N \ , \tag{9}$$

where $n$ is the real part of the refractive index and $n_g$ is the group index. The mode dependence of $\Delta v$ is given predominantly by the wavelength-dependence of $dn'/dN$. If the instantaneous frequency of the electric field, $E(t)$, of each longitudinal mode is $v + \Delta v$, then the electric field can be written as

$$E(t) = E_0(t)\, e^{i\psi(t)} \ , \tag{10}$$

where the rate of change of phase is given by

$$\psi = 2\pi(\nu + \Delta\nu) \ . \tag{11}$$

The electric field under small signal sinusoidal modulation at frequency ω is given by

$$E(t) = E_0 e^{i\left(2\pi\nu t + \beta\cos\omega t\right)} \ , \tag{12}$$

where β is the FM index and is given by

$$\beta = 2\pi\left|\int \Delta\nu(t)dt\right| \ . \tag{13}$$

Using equations (8), (9), and (13) we can obtain

$$\left(\frac{\beta\omega}{m}\right)^2 = \left(\frac{\alpha}{2}\right)^2(\omega^2 + \gamma_n^2) \ , \tag{14}$$

where $m$ is the AM index given by $m = |\Delta S/S|$ and α is defined as $(4\pi/\lambda)\cdot(dn'/dN)(dG/dN)$. The total photon density modulation, $\Delta S$, is involved in the amplitude modulation index because the carrier density modulation, $\delta N$, is described by $\Delta S$ as in equation (8). The quantities α and β can be wavelength dependent (mode dependent) through the wavelength dependence of $dn'/dN$.

# 4. Results and Discussion

The frequency-modulated optical wave is represented by

$$E = E_0\, e^{(j\,[2\pi f_0 t + \beta\sin(2\pi f_m t)])},$$

where

$$\beta = \frac{\Delta F}{f_m} \ ,$$

$f_0$ is the center frequency, $\Delta F$ is the maximum frequency deviation, $f_m$ is the modulation frequency, and β is the frequency modulation index. The laser diode has a particular threshold current ($I_{th}$) of about 40 mA maximum, with the single longitudinal mode wavelength at 1.35 μm and a typical lasing wavelength of 1.30 μm, which was found to be the case in our spectral

analysis. The lasing spectra under various dc current values are given in figure 2.

The multimode spectrum due to spontaneous emission shows maximum peak intensity for a dc current of 115 mA. The semiconductor laser behaves as a regenerative noise amplifier [14] and all modes for which the round-trip gain is positive are amplified. Once the threshold is reached, the gain is approximately clamped, and power in the side mode saturates. In this model [15] the mode suppression ratio (ratio of main mode power to power of most intense side mode) increases continuously with an increase in the laser power. However, with an increase in the laser power, not only does the longitudinal mode move across the gain curve, but also several other phenomena, such as spatial and spectral hole burning, can start to influence the longitudinal mode behavior.

According to equation (12) the amplitude and phase of the optical field undergo sinusoidal modulation when an rf current is applied to the laser. This simultaneous change in phase or frequency modulation is governed by the linewidth enhancement factor and its origin in the index change that invariably occurs when the optical gain changes in response to variations in the carrier population. In the experiment the free spectral range (FSR) of the FP was 15 GHz with a finesse greater than 60. In the seven pictures in figure 3, observations can be made about the changes in the spectrum as the modulation depth is increased in steps.

Figure 3(a) shows the laser spectra with no modulation input to the driver. The three peaks are successive longitudinal modes of the FP as one end plate is mechanically vibrated. We obtain the high resolution spectrum by selectively choosing it at a longitudinal mode and then scanning through the FP and optically detecting and analyzing with a fast oscilloscope. For the rest of the pictures, sinusoidal modulation at a frequency of 8 GHz has been applied at various power levels as indicated. Figure 3(g) demonstrates clearly frequency modulation of the laser since the carrier gets completely suppressed. This is frequency modulation with an index of 2.3, corresponding to the first zero-order Bessel function.

The intensity of the zero-order sideband under modulation is given by

$$\left|J_0(\beta)\right|^2 + \left|(\overline{m}/2)\,J_1(\beta)\right|^2 ,$$

where $J_0$ and $J_1$ are Bessel functions and $\overline{m}$ is the amplitude modulation index of that particular mode. For the small signal modulation the intensity of the zero-order sideband is well approximated by $|J_0(\beta)|^2$. If the modulation is absent, the intensity is given by $|J_0(0)|^2$. Thus the measurement of the zero-order sideband intensity ratio with and without modulation allows index $\beta$ calculation if $m$ is small. If so, then absence of amplitude modulation can be seen on the detector without a spectrum analyzer. This experimental result shows that the effect of current modulation of the laser results at first in frequency modulation of the output, and only with further increase in modulation drive level and/or readjustment of the laser bias current does

(a)

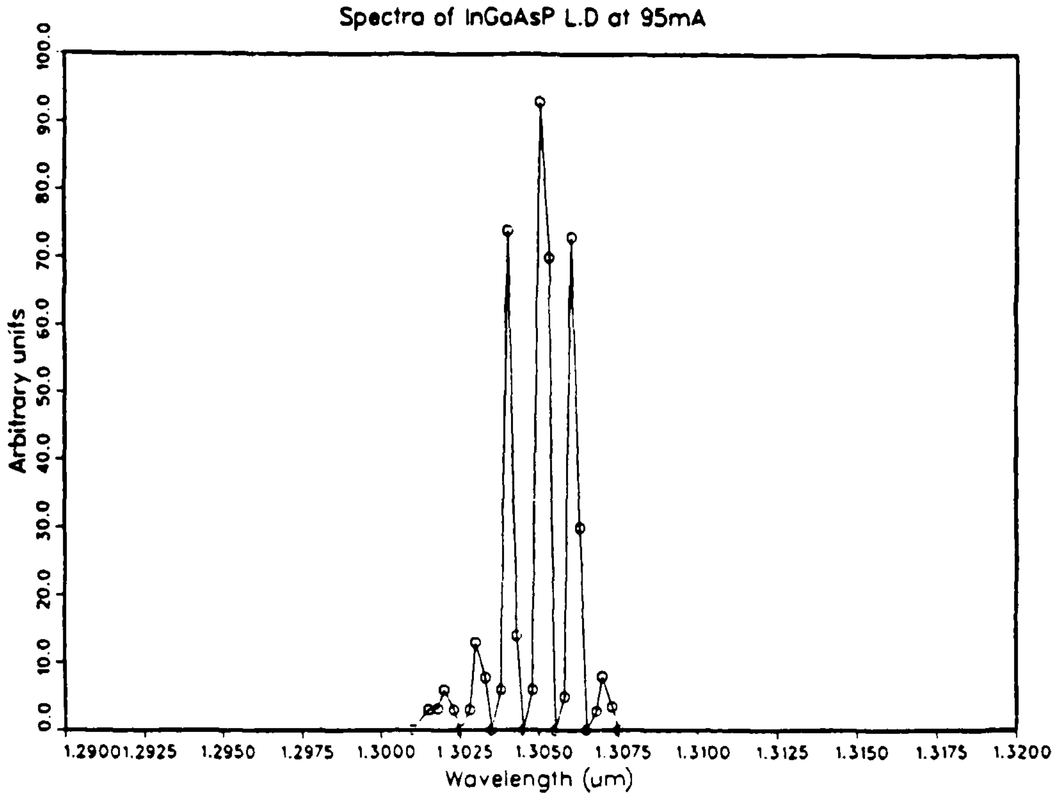


(b)

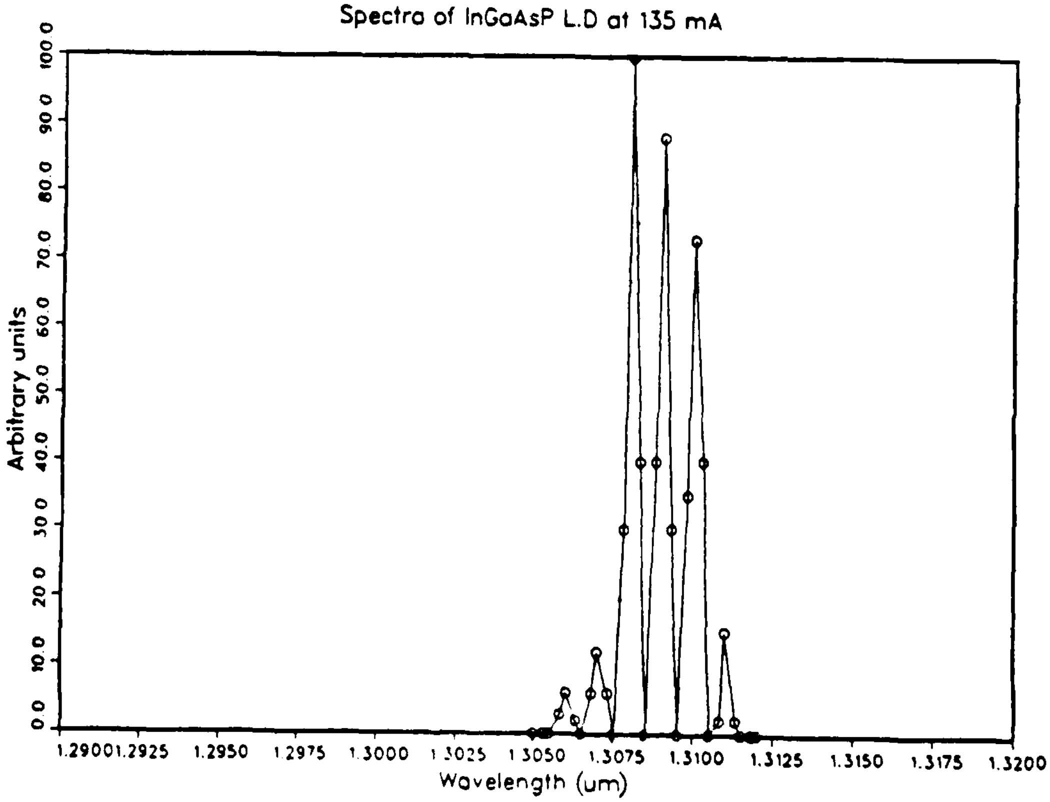


**Figure 2. Observed spectra of InGaAsP laser for various dc currents.**

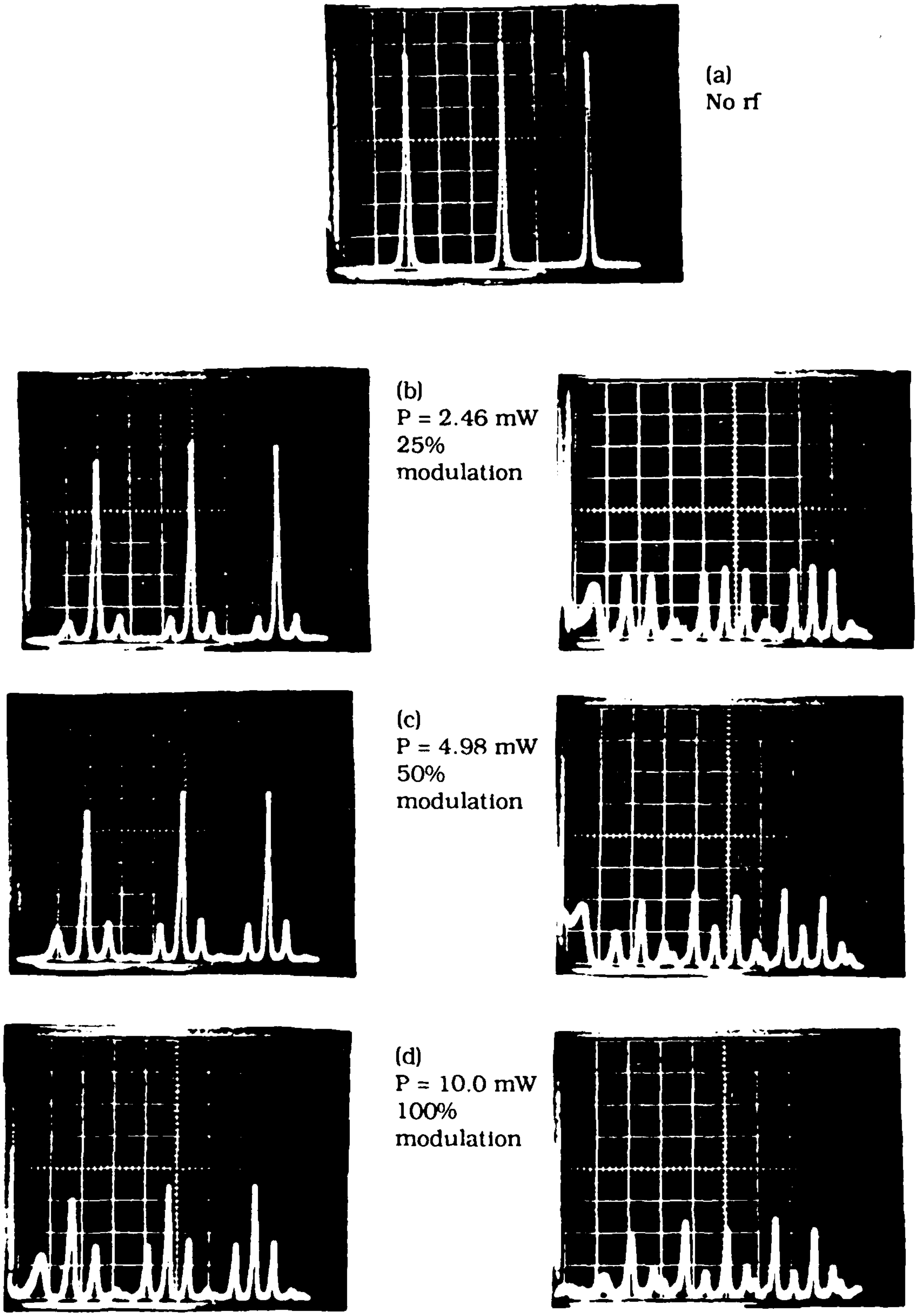

(a)
No rf

(b)
P = 2.46 mW
25%
modulation

(c)
P = 4.98 mW
50%
modulation

(d)
P = 10.0 mW
100%
modulation

(e)
P = 14.97 mW
150%
modulation

(f)
P = 19.95 mW
200%
modulation

(g)
P = 25.0 mW
250%
modulation

**Figure 3. Spectra of frequency modulated InGaAsP laser: $I_{dc}$ = 135 mA, $\lambda_0$ = 1.30 μm, FSR = 15 GHz.**

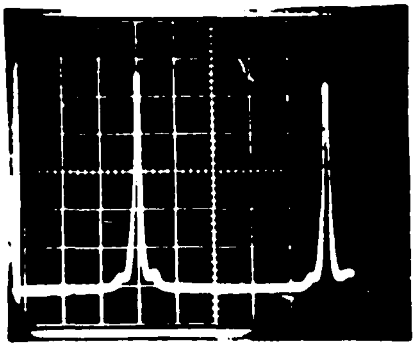

(a)
4 GHz

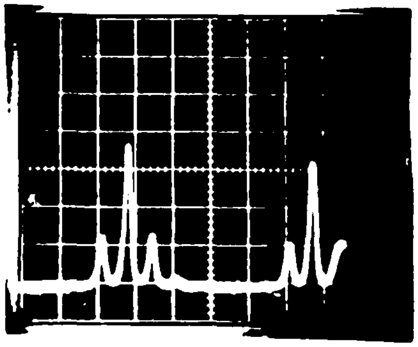

(b)
6 GHz

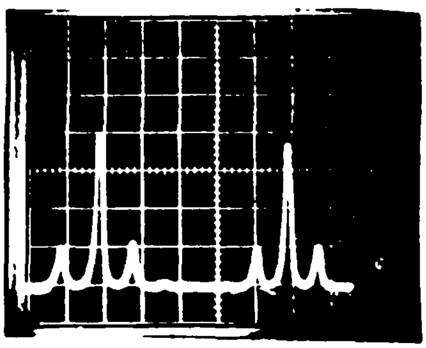

(c)
8 GHz

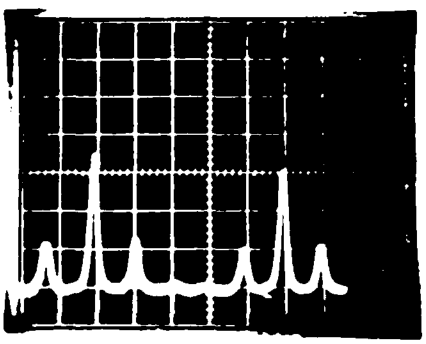

(d)
10 GHz

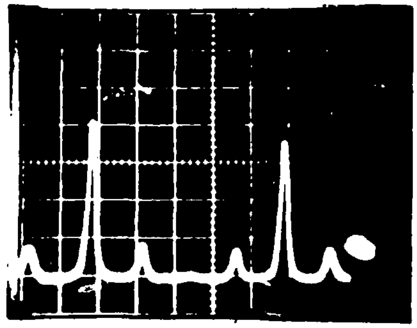

(e)
12 GHz

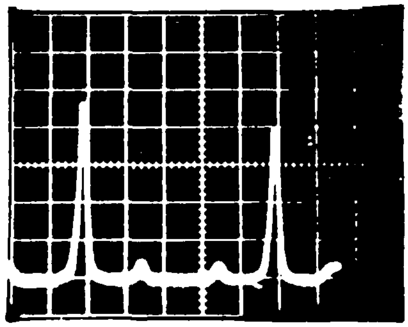

(f)
14 GHz

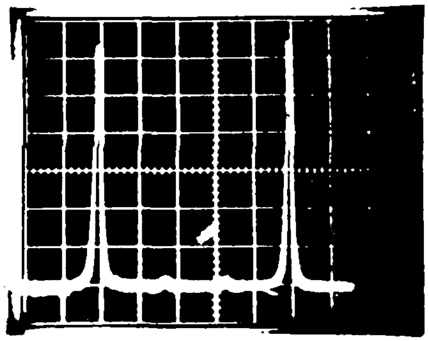

(g)
16 GHz

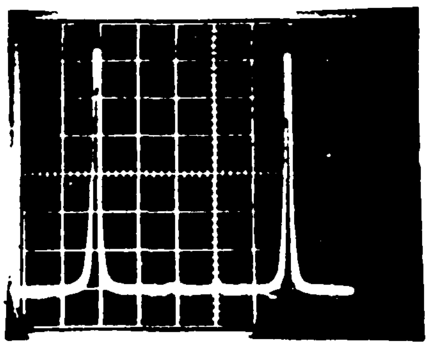

(h)
18 GHz

**Figure 4. Spectra of InGaAsP laser with frequency modulation: $I_{dc}$ = 115 mA, FSR = 15 GHz, rf power = 5 mW. Here rf frequencies are changed from 4 to 18 GHz in steps of 2 GHz.**

modulation drive level and/or readjustment of the laser bias current does amplitude modulation occur.

In another experiment modulation frequencies were varied after the rf power being applied was kept constant for a frequency modulation index of 0.50. The results are shown in figure 4.

It can be seen clearly that frequency modulation increases up to 10 GHz, then decreases for higher frequency of modulation. These changes, which can be clearly seen, may be due to the nonlinear gain term in equation (3) so there might be changes occurring in the carrier density and refractive index. Although the present frequency modulation measurement does not identify the physical mechanism for the nonlinear gain, it does provide some accurate ways to analyze the modulation indexes.

# 5. Conclusions

We have demonstrated a high-resolution spectral measurement setup which has allowed us to successfully observe frequency modulation properties of a buried heterostructure 1.3-μm InGaAsP injection laser. Frequency modulation up to 8 GHz with a modulation index of 2.4 has been demonstrated. The number of lasing modes increased with increasing modulation depth, especially beyond 100-% modulation depth. Also, direct modulation of the same laser was performed up to 18 GHz with an rf power of 5 mW, and it was observed that the frequency modulation index went from 0.7 to nearly 0 as the modulation frequency was increased. These measurements indicate that the nonlinear gain effects mainly influence the modulation characteristics of this semiconductor laser. The smaller damping factor of a multi-longitudinal laser compared to that of a single longitudinal mode laser suggests that wider maximum bandwidths and modulation indexes can be achieved in multimode devices. Also for this laser, for higher drive currents the spectrum remains multimode with strong sidebands. However, sidemode suppression may not be an important criterion for high-frequency modulation. Currently this laser is the fastest (= 23 GHz) on the market.

# References


1. R. Olshansky, W. Powazinik, P. Hill, V. Lanziera, and R. B. Lauer, InGaAsP Buried Heterostructure Laser with 22 GHz Bandwidth and High Modulation Efficiency, *Electron. Lett*, **23**(16) (1987), 239.

2. Fred Semendy and Emanuel Katzen, Microwave Fiberoptic Links for Phased Arrays, *SPIE Proc.*, **886**, Los Angeles (Jan. 1988), 247.

3. T. Ikegami, Spectrum Broadening and Tailing Effect in Directly Modulated Injection Lasers, *Technical Digest*, 1st European Conf. Opt. Fibre Commun (1975), 111.

4. J. M. Osterwalder and R. J. Rickett, Frequency Modulation of GaAlAs Injection Lasers at Microwave Frequency Rate, *IEEE J. Quantum Electron*, **QE-16** (1980), 250.

5. S. Kobayashi, Y. Yamamoto, and T. Kimura, Modulation Frequency Characteristics of Directly Optical Frequency Modulated AlGaAs Semiconductor Laser, *Electron. Lett*, **17** (1981), 350.

6. Y. Yamamoto and T. Kimura, Coherent Optical Fiber Transmission Systems, *IEEE J. Quantum Electron.*, **QE-17** (1981), 919.

7. D. Marcuse and T. P. Lee, On Approximate Analytical Solution of Rate Equations for Studying Transient Spectra of Injection Lasers, *IEEE J. Quantum Electron.*, **QE-19** (1983), 1397.

8. H. Satz and G. deMars, Transients and Oscillation Pulses in Masers, *Quantum Electronics*, C. H. Townes, ed., New York, Columbia University Press (1960), 530.

9. C. B. Su and V. A. Lanziera, Ultra High Speed Modulation of 1.3 mm InGaAsP Diode Laser, *IEEE J. Quantum Electron.*, **QE-22** (1986), 1568.

10. D. J. Chanin, Effect of Gain Saturation on Injection Laser Switching, *J. Appl. Phys.*, **50** (1979), 3858.

11. R. S. Tucker and D. J. Pope, Circuit Modeling of the Effect of Diffusion on Damping in a Narrow Stripe Semiconductor Laser, *IEEE J. Quantum Electron.*, **QE-19** (1983), 1179.

12. R. S. Tucker and K. P. Kaminov, High Frequency Characteristics of Directly Modulated InGaAsP Ridge Waveguide Buried Heterostructure Laser, *J. Lightwave Technol.*, **LT-2** (1984), 385.

13. C. H. Henry, Theory of Linewidth of Semiconductor Lasers, *IEEE J. Quantum Electron.*, **QE-18** (1982), 259.

14. E. I. Gordon, Bell Syst Tech. J., **43** (1964), 507.

15. T. P. Lee, C. A. Barrus, J. A. Copeland, A. G. Dentai, and D. Marcuse, *IEEE J. Quantum Electron.*, **QE-18** (1982), 1101.

DISTRIBUTION

ADMINISTRATOR
DEFENSE TECHNICAL INFORMATION CENTER
ATTN DTIC-DDA (12 COPIES)
CAMERON STATION, BUILDING 5
ALEXANDRIA, VA 22314

DIRECTOR
DEFENSE ADVANCED RESEARCH PROJECTS AGENCY
ATTN J. FRIEBELE
1400 WILSON BLVD
ARLINGTON, VA 22209

DIRECTOR
DEFENSE NUCLEAR AGENCY
ATTN TECH LIBRARY
WASHINGTON, DC 20305

UNDER SECRETARY OF DEFENSE RES & ENGINEERING
ATTN TECHNICAL LIBRARY, 3C128
WASHINGTON, DC 20301

OFFICE OF THE ASSIST SEC OF THE ARMY (RDA)
ATTN DAMA-ARZ-B, I. R. HERSHNER
WASHINGTON, DC 20310

COMMANDER
US ARMY ARMAMENT MUNITIONS & CHEMICAL COMMAND (AMCCOM)
US ARMY ARMAMENT RESEARCH & DEVELOPMENT CENTER
ATTN DRDAR-TSS, STINFO DIV
DOVER, NJ 07801

COMMANDER
ATMOSPHERIC SCIENCES LABORATORY
ATTN TECHNICAL LIBRARY
WHITE SANDS MISSILE RANGE, NM 88002

DIRECTOR
US ARMY BALLISTIC RESEARCH LABORATORY
ATTN SLCBR-DD-T (STINFO)
ABERDEEN PROVING GROUND, MD 21005

DIRECTOR
US ARMY ELECTRONICS WARFARE LABORATORY
ATTN J. CHARLTON
ATTN DELET-DD
FT MONMOUTH, NJ 07703

COMMANDING OFFICER
USA FOREIGN SCIENCE & TECHNOLOGY CENTER
FEDERAL OFFICE BUILDING
ATTN DRXST-BS, BASIC SCIENCE DIV
CHARLOTTESVILLE, VA 22901

COMMANDER
US ARMY MATERIALS & MECHANICS RESEARCH CENTER
ATTN DRXMR-TL, TECH LIBRARY
WATERTOWN, MA 02172

US ARMY MATERIEL COMMAND
5001 EISENHOWER AVE
ALEXANDRIA, VA 22333-0001

COMMANDER
US ARMY MISSILE & MUNITIONS CENTER & SCHOOL
ATTN ATSK-CTD-F
ATTN DRDMI-TB, REDSTONE SCI INFO CENTER
REDSTONE ARSENAL, AL 35809

DIRECTOR
NIGHT VISION & ELECTRO-OPTICS LABORATORY
ATTN TECHNICAL LIBRARY
ATTN A. BYONG
ATTN R. BUSER
ATTN C. FREEMAN
ATTN J. HABERSAT
ATTN M. NORTON
ATTN A. PINTO
ATTN J. POHLMANN
ATTN J. POLLARD
ATTN P. AMIRTHA RAS
ATTN J. RATCHES
ATTN R. ROHDY
ATTN E. SHARP
ATTN S. SONSTROEM
ATTN B. SPANDE
ATTN W. TRUSSELL
ATTN G. WOOD
FT BELVOIR, VA 22060

COMMANDER
CENTER FOR NIGHT VISION & ELECTRO-OPTICS
ATTN F. SEMENDY, AMSEL-RD-NV-LO (20 COPIES)
FT BELVOIR, VA 22060

COMMANDER
US ARMY RESEARCH OFFICE
(DURHAM)
PO BOX 12211
ATTN R. J. LONTZ
ATTN M. STROSIO
ATTN M. CIFTAN
ATTN B. D. GUENTHER
ATTN C. BOGOSIAN
RESEARCH TRIANGLE PARK, NC
27709

COMMANDER
US ARMY RSCH & STD GRP (EUROPE)
FPO NEW YORK 09510

COMMANDER
US ARMY TEST & EVALUATION
COMMAND
ATTN D. H. SLINEY
ATTN TECH LIBRARY
ABERDEEN PROVING GROUND, MD
21005

COMMANDER
US ARMY TROOP SUPPORT COMMAND
ATTN DRXRES-RTL, TECH LIBRARY
NATICK, MA 01762

OFFICE OF NAVAL RESEARCH
ATTN J. MURDAY
ARLINGTON, VA 22217

DIRECTOR
NAVAL RESEARCH LABORATORY
ATTN CODE 2620, TECH LIBRARY BR
ATTN CODE 5554, F. BARTOLI
ATTN CODE 5554, L. ESTEROWITZ
ATTN CODE 5554, R. E. ALLEN
ATTN L. GOLDBERG
ATTN M. PARENT
WASHINGTON, DC 20375

COMMANDER
NAVAL WEAPONS CENTER
ATTN CODE 3854, R. SCHWARTZ
ATTN CODE 3854, M. HILLS
ATTN CODE 3844, M. NADLER
ATTN CODE 385, R. L. ATKINS
ATTN CODE 343, TECHNICAL
INFORMATION DEPARTMENT
CHINA LAKE, CA 93555

AIR FORCE OFFICE OF SCIENTIFIC
RESEARCH
ATTN MAJOR H. V. WINSOR, USAF
BOLLING AFB
WASHINGTON, DC 20332

HQ, USAF/SAMI
WASHINGTON, DC 20330

NASA/LEWIS RESEARCH CENTER
ATTN K. BHASIV
2100 BROOK PARK ROAD
CLEVELAND, OH 44135

DEPARTMENT OF COMMERCE
NATIONAL BUREAU OF STANDARDS
ATTN LIBRARY
WASHINGTON, DC 20234

DIRECTOR
ADVISORY GROUP ON ELECTRON DEVICES
ATTN SECTRY, WORKING GROUP D
201 VARICK STREET
NEW YORK, NY 10013

AEROSPACE CORPORATION
PO BOX 92957
ATTN M. BIRNBAUM
ATTN N. C. CHANG
LOS ANGELES, CA 90009

ALLIED
ADVANCED APPLICATION DEPT
ATTN A. BUDGOR
31717 LA TIEMDA DRIVE
WESTLAKE VILLAGE, CA 91362

AMES LABORATORY DOE
IOWA STATE UNIVERSITY
ATTN K. A. GSCHNEIDNER, JR. (2 COPIES)
AMES, IA 50011

ARGONNE NATIONAL LABORATORY
ATTN W. T. CARNALL
9700 SOUTH CASS AVENUE
ARGONNE, IL 60439

BDM CORPORATION
ATTN R. ATHALE
MC LEAN, VA 22180

BRIMROSE CORP OF AMERICA
ATTN R. G. ROSEMEIER
7527 BELAIR ROAD
BALTIMORE, MD 21236

CORNING GLASS WORKS
ATTN J. WAHL
CORNING, NY 14831

ENGINEERING SOCIETIES LIBRARY
ATTN ACQUISITIONS DEPT
345 EAST 47TH STREET
NEW YORK, NY 10017

DISTRIBUTION (cont'd)

GTE LABS
ATTN R. OLSHANSKY
ATTN U. LANZIERA
ATTN W. POWAZINIK
ATTN R. B. LAUER
40 SYLVAN ROAD
WALTHAM, MA 02254

IBM RESEARCH DIVISION
ALMADEN RESEARCH CENTER
ATTN R. M. MACFARLANE
MAIL STOP K32 802(D)
650 HARRY ROAD
SAN JOSE, CA 95120

DIRECTOR
LAWRENCE RADIATION LABORATORY
ATTN M. J. WEBER
ATTN H. A. KOEHLER
ATTN W. KRUPKE
LIVERMORE, CA 94550

MARTIN MARIETTA
ATTN F. CROWNE
ATTN J. LITTLE
ATTN T. WORCHESKY
ATTN D. WORTMAN
1450 SOUTH ROLLING ROAD
BALTIMORE, MD 21227

MIT LINCOLN LAB
ATTN B. AULL
PO BOX 73
LEXINGTON, MA 02173

DEPARTMENT OF MECHANICAL, INDUSTRIAL,
& AEROSPACE ENGINEERING
ATTN S. TEMKIN
PO BOX 909
PISCATAWAY, NJ 08854

NATIONAL OCEANIC & ATMOSPHERIC ADM
ENVIRONMENTAL RESEARCH LABS
ATTN LIBRARY, R-51, TECH RPTS
BOULDER, CO 80302

OAK RIDGE NATIONAL LABORATORY
ATTN R. G. HAIRE
OAK RIDGE, TN 37830

ORTEL CORPORATION
ATTN K. Y.. LAU
ATTN B. CHAIM
ATTN I. URY
ALHAMBRA, CA 91803

ROME AIR DEVELOPMENT CENTER
ATTN P. SIRAK
ATTN B. HENDRICKSON
ROME, NY

SCIENCE APPLICATIONS, INC
ATTN T. ALLIK
1710 GOODRIDGE DRIVE
McLEAN, VA 22102

UNION CARBIDE CORP
ATTN M. R. KOKTA
ATTN J. H. W. LIAW
750 SOUTH 32ND STREET
WASHOUGAL, WA 98671

ARIZONA STATE UNIVERSITY
DEPT OF CHEMISTRY
ATTN L. EYRING
TEMPE, AZ 85281

CALTECH
ATTN A. YARIV
WATSON 128-95
PASADENA, CA 91125

CARNEGIE MELLON UNIVERSITY
SCHENLEY PARK
ATTN PHYSICS & EE, J. O. ARTMAN
ATTN D. CASASENT, B.V.K.V. KUMAR
PITTSBURGH, PA 15213

COLORADO STATE UNIVERSITY
PHYSICS DEPARTMENT
ATTN S. KERN
FORT COLLINS, CO 80523

DREXEL UNIVERSITY
DEPT OF ELEC ENGINEERING
ATTN P. R. HERCZEFELD
ATTN A. S. DARYOUSH
PHILADELPHIA, PA 19104

JOHNS HOPKINS UNIVERSITY
DEPT OF PHYSICS
ATTN B. R. JUDD
BALTIMORE, MD 21218

HOWARD UNIVERSITY
DEPTARTMENT OF CHEMISTRY
ATTN J. NICHOLSON
ATTN R. BUTCHER
ATTN M. KRISHNAMURTHY
WASHINGTON, DC

MASSACHUSETTS INSTITUTE OF
TECHNOLOGY
CRYSTAL PHYSICS LABORATORY
ATTN H. P. JENSSEN
ATTN A. LINZ
CAMBRIDGE, MA 02139

MASSACHUSETTS INSTITUTE OF
TECHNOLOGY
ATTN V. BAGNATO
77 MASS AVE
ROOM 26-251
CAMBRIDGE, MA 02139

UNIVERSITY OF MARYLAND
DEPT OF ELECTRICAL ENGINEERING
ATTN CHI. H. LEE
ATTN M. DAGENEU
ATTN RAJ KHANNA (CHEMISTRY)
COLLEGE PARK, MD

UNIVERSITY OF MICHIGAN
DEPT OF ELECTRICAL ENGINEERING
ATTN P. BHATTACHARYA
ATTN J. SINGH
ATTN G. HADDAD
ANN ARBOR, MI 48104

OKLAHOMA STATE UNIVERSITY
DEPT OF PHYSICS
ATTN R. C. POWELL
STILLWATER, OK 74078

PENNSYLVANIA STATE UNIVERSITY
MATERIALS RESEARCH LABORATORY
ATTN W. B. WHITE
UNIVERSITY PARK, PA 16802

SAN JOSE STATE UNIVERSITY
DEPARTMENT OF PHYSICS
ATTN J. B. GRUBER
SAN JOSE, CA 95192

US ARMY LABORATORIES COMMAND
ATTN TECHNICAL DIRECTOR, AMSLC-CT

INSTALLATION SUPPORT ACTIVITY
ATTN LEGAL OFFICE, SLCIS-CC
ATTN S. ELBAUM, SLCIS-CC-IP

USAISC
ATTN RECORD COPY, AMSLC-IM-TS
ATTN TECHNICAL REPORTS BRANCH,
AMSLC-IM-TR (2 COPIES)

HARRY DIAMOND LABORATORIES
ATTN D/DIVISION DIRECTORS
ATTN LIBRARY, SLCHD-TL (3 COPIES)
ATTN LIBRARY, SLCHD-TL (WOODBRIDGE)
ATTN CHIEF, SLCHD-NW-E
ATTN CHIEF, SLCHD-NW-EH
ATTN CHIEF, SLCHD-NW-EP
ATTN CHIEF, SLCHD-NW-ES

HARRY DIAMOND LABORATORIES
(cont'd)
ATTN CHIEF, SLCHD-NW-R
ATTN CHIEF, SLCHD-NW-CS
ATTN CHIEF, SLCHD-NW-RP
ATTN CHIEF, SLCHD-NW-RS
ATTN CHIEF, SLCHD-NW-TN
ATTN CHIEF, SLCHD-NW-TS
ATTN CHIEF, SLCHD-NW-P
ATTN CHIEF, SLCHD-PO
ATTN CHIEF, SLCHD-ST-C
ATTN CHIEF, SLCHD-ST-AP
ATTN CHIEF, SLCHD-ST-OP
ATTN CHIEF, SLCHD-ST-RS
ATTN CHIEF, SLCHD-ST-SS
ATTN CHIEF, SLCHD-TT
ATTN WALTER, SANDRA, SLCIS-CP-TD
ATTN WILLIS, B., SLCHD-IT-EB
ATTN HERSHALL, P., SLCHD-MI-S
ATTN KENYON, C. S., SLCHD-NW-EP
ATTN MILETTA J. R., SLCHD-NW-EP
ATTN McLEAN, F. B., SLCHD-NW-RP
ATTN SATTLER, J., SLCHD-PO-P
ATTN BAHDER, T., SLCHD-ST-AP
ATTN BRODY, P., SLCHD-ST-AP
ATTN BRUNO, J., SLCHD-ST-AP
ATTN DROPKIN, H., SLCHD-ST-AP
ATTN EDWARDS, SLCHD-ST-AP
ATTN HANSEN, A., SLCHD-ST-AP
ATTN HAY, G., SLCHD-ST-AP
ATTN KATZEN, E., SLCHD-ST-AP
ATTN MORRISON, C., SLCHD-ST-AP
ATTN NEIFELD, R., SLCHD-ST-AP
ATTN PENNISE, C., SLCHD-ST-AP
ATTN SCHMALBACH, R., SLCHD-ST-AP
ATTN SIMONIS, G., SLCHD-ST-AP
ATTN STELLATO, J., SLCHD-ST-AP
ATTN TOBIN, M., SLCHD-ST-AP
ATTN TOBER, R., SLCHD-ST AP
ATTN TURNER, G., SLCHD-ST-AP
ATTN WONG, B., SLCHD-ST-AP
ATTN WORTMAN, D., SLCHD-ST-AP
ATTN LIBELO, L., SLCHD-ST-MW
ATTN GARVIN, C., SLCHD-ST-OP
ATTN GUPTA, N., SLCHD-ST-OP
ATTN MASLOWE, B., SLCHD-ST-OP
ATTN HARRISON, L., SLCHD-ST-OP
ATTN SCHOCKLEY, D., SLCHD-ST-OP
ATTN WEBER, B., SLCHD-ST-R
ATTN BENCIVENGA, A. A., SLCHD-ST-RP
ATTN STEAD, M., SLCHD-ST-RP
ATTN NEMARICH, J., SLCHD-ST-SP
ATTN Z. G. SZTANKAY, SLCHD-ST-SP
ATTN GOFF, J., SLCHD-ST-SS
ATTN BENCIVENGA B., SLCHD-TA-AS